BACKSCATTER PROPERTIES OF MULTITEMPORAL TERRASAR-X DATA AND THE EFFECTS OF INFLUENCING FACTORS ON BURN SEVERITY EVALUATION, IN A MEDITERRANEAN PINE FOREST

Mihai Tanase (1), Maurizio Santoro (2), Juan de la Riva (1) and Fernando Pérez-Cabello (1)

(1) University of Zaragoza, Dpt. of Geography, Pedro Cerbuna 12, 50009, Zaragoza, Spain
(2) Gamma Remote Sensing AG, Worbstrasse 225, CH-3073 Gümligen, Switzerland

ABSTRACT

TerraSAR-X dual-polarized (HH and HV polarization) backscatter data have been investigated to assess the temporal backscatter stability of a burn scar in Spain. Analysis of the main factors influencing burn severity evaluation has been also carried out. The temporal stability of the backscatter was strong, unburned areas showing differences of less than 0.6 dB. For increasing burn severity the backscatter varied by up to 2 dB in highly burned areas located on slopes tilted towards the sensor. Heavy rainfall or moist vegetation increased the backscatter up to 1 dB. Steeper look angles resulted in significantly higher backscatter coefficients for HH polarization, while for HV polarization only marginal increase was observed. Association strength between backscatter and burn severity estimates improved with the size of the multi-look window, at the expenses however of spatial resolution. Even better results could be achieved at higher spatial resolution by applying a multi-temporal speckle filtering algorithm.

Index Terms— burn severity, Terrasar-X, backscatter

1. INTRODUCTION

Forest fires are an important source of atmospheric aerosols and green-house gasses, causal relationship between biomass burning and inter-annual variability of related emissions being observed [1]. The duration and intensity of a fire determines not only the quantity of the green-house gasses and aerosols emissions [2] but also the recovery processes years after the event. Burn severity is nowadays used to express fire effects on ecosystems and is defined as the degree of the environmental changes caused by fire. One of the most widely employed optical-based spectral indexes for burn severity assessment is the Normalized Burn Ratio (NBR) [3] used in a bi-temporal approach with pre- and post-fire datasets (dNBR). dNBR provides a scale of changes with respect to the pre-fire status, unburned area retaining values close to zero (i.e. little or no change). Nevertheless, reflectance based indexes often fail to produce accurate results especially for intermediate burn severity levels where multiple effects combine. Most studies found it problematic to discriminate intermediate burn severities [4].

An alternative method for burn severity estimation is the use of synthetic aperture radar (SAR) images since they contain information related to forest structure, removal of leaves and branches by fire directly influencing the radar backscatter. Previous work confirmed the utility of SAR data for remote estimation of burned areas [5]. Statistically significant relations have been found between TerraSAR-X (X-band) HH and HV polarizations and burn severity when both channels were used in linear regression models [6]. To further assess the capability of TerraSAR-X backscatter to map burn severity, the temporal stability and the backscatter response over a burned area for data acquired at different look angles and under variable weather condition were investigated. The radar signal is influenced by viewing geometry (i.e. look angle), soil and vegetation moisture and ephemeral effects of forests (e.g. changes in leaf orientation due to wind). Consequently, backscatter coefficient could increase or decrease as a function of other factors such as vegetation type, structure, orientation etc. Because of the high resolution of the data, we could also investigate the effect of speckle reduction techniques (spatial multi-looking and multi-temporal filtering) on the association strength between the backscatter and burn severity.

2. STUDY AREA AND DATA SETS

The Zuera study area is located in central Ebro Valley and has a semi-arid mediterranean climate with continental characteristics and marked seasonal precipitation variations. Most of the area is covered by homogeneous, even aged pine forests of *Pinus halepensis L.* interspersed with agricultural fields. The forest fire under investigation occurred between 6-16th August, 2008 after a traffic accident and burned approximately 2200 ha of vegetation.

The dataset consisted of seven TerraSAR-X (TSX) and one pair of Landsat 5 TM images. Dual polarization TSX data were acquired between November 2008 and March 2009 in Stripmap (SM) mode at look angles of 25° and 40°. The six SAR images acquired at 40° look angle were calibrated and then multi-looked with two sets of factors in order to obtain images at different spatial resolutions (10 and 25 m pixel spacing). Subsequently, the images were co-registered, achieving sub-pixel accuracy, using a cross-correlation algorithm based on intensity tracking [7]. Adaptive multi-temporal filtering (AdMTF) [8] was carried out at both spatial resolutions using stacks of three and six co-registered images. The ENL after multi looking and temporal filtering together with the main SAR data characteristics and processing parameters are presented in Table I. The image acquired at 25° was processed to 25 m spatial resolution. All images were geocoded to UTM projection using a digital elevation model (DEM) with 20 m pixel spacing. Detailed information on SAR geocoding process is given in [6]. Topographic normalization for the varying incidence angle and effective pixel area was applied [9] using information derived from the DEM. All resulting images, obtained in gamma nought (γ°) format, were scaled to the look angle at mid swath.

The Landsat scenes (path 199, row 031) were acquired on July 21st (pre-fire) and August 22nd, 2008 (post-fire). Subsets of the scenes were geometrically rectified to the same coordinate system as SAR data using a linear polynomial model and incorporating information of the local topography [6]. Landsat TM data were used to derive optical based estimates (dNBR) of burn severity.

TABLE I
SAR DATA CHARACTERISTICS AND PROCESSING PARAMETERS – SUMMARY

Parameter	Value
Acquisition dates for 40° look angle data	2008.11.16 / 2008.12.19 / 2009.01.21 / 2009.02.12 / 2009.02.23 / 2009.03.06
Acquisition date for 25° look angle data	2008.12.24
SSC pixel spacing (slant range, azimuth)	0.91 m × 2.43 m
Multi-look factors (range pixels, azimuth pixels)	a) 17 × 10, b) 8 × 5
ML images pixel spacing (slant range, azimuth)	a) 15.5 m × 24.3 m, b) 7.3. m × 12.1 m
Pixel spacing of geocoded images	a) 25 m × 25 m, b) 10 m × 10 m
ENL (25 m spatial resolution)	no AdTMF: 55 / AdMTF using 3 images: 90 / AdMTF using 6 images: 125
ENL (10 m spatial resolution)	no AdMTF: 9 / AdMTF 3 using images: 25 / AdMTF using 6 images: 32

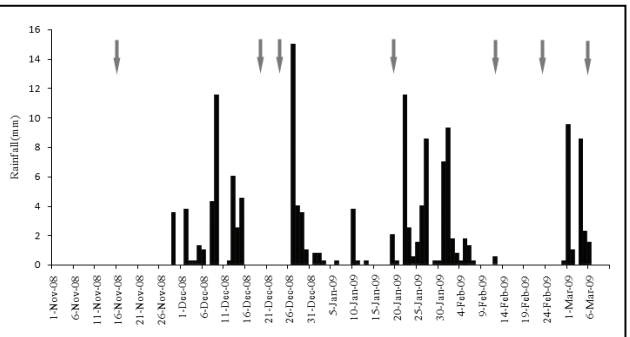

Fig. 1 Daily precipitation and image acquisition dates (arrows)

For the interpretation of backscatter signatures precipitation recorded during the period of image acquisitions (Figure 1) was obtained from an automatic rain gauge installed roughly at the center of the fire perimeter.

3. METHODS

Backscatter temporal trends, weather and viewing geometry effects on backscatter coefficient were analyzed using descriptive statistics (i.e. mean backscatter values by groups of local incidence angle). To evaluate the performance of speckle suppression methods linear regression analysis was employed. Since multiple regression requires large number of samples which cannot be easily achieved by field work the investigation was carried out using a set of automatically generated pseudo-plots. Pseudo-plots were generated by averaging pixels of similar burn severity (i.e. dNBR) for the same local incidence angle rounded to unity. To avoid possible bias only pseudo-plots containing a specific number of pixels (i.e. 4, 9, 10, 16, 25 and 50) were selected. High determination coefficient were found between field estimates of burn severity by means of Composite Burn Index (CBI) and dNBR ($R^2 = 0.81$, $P<0.05$). This result supported the assumption that dNBR can be considered for further use as a radiometric index strongly related to the severity levels recorded in the field. Detailed information on pseudo-plots generation and CBI assessment is given in [6].

Determination coefficients (R^2) were used to relate SAR data to optical sensor based estimates (dNBR) of burn severity. Multiple linear regression analysis was employed after grouping pseudo-plots in 5° intervals of local incidence angle to evaluate the association strength between burn severity and radar backscatter. Regression analysis was carried out using 900 randomly selected pseudo-plots. The effect of speckle reduction techniques on burn severity estimates were assessed using pseudo-plots formed by 10, 25 and 50 pixels for data geocoded to 10 m pixel spacing and by 4, 9 and 16 pixels for data geocoded to 25 m pixel spacing.

4. RESULTS AND DISCUSSION

4.1. Backscatter signatures in relation to weather conditions and image viewing geometry

The backscatter signatures at HH and HV polarizations are presented in Figure 2 for the images acquired at 40° look angle. To minimize the effect of topography the averages were calculated for groups of local incidence angles from data geocoded at 10 m pixel spacing using 0.1 ha (i.e. 10 pixels) pseudo-plots. For unburned areas the backscatter was rather constant in time, the variation being within the absolute radiometric accuracy (0.6 dB). For a given severity, the backscatter coefficient varied by 1-2 dB, larger variations being observed for high burn severity levels at both polarizations. This can be explained by taking into account that at higher burn severity levels soil exposure increases; hence, soil roughness and soil moisture induce larger backscatter variations. For smaller local incidence angles (i.e. slopes oriented towards the sensor) the spread increased slightly while for larger local incidence angles (i.e. slopes oriented away from sensor) the maximum spread showed a certain decrease when compared to flat or near flat areas (i.e. 35-45° local incidence angle). This behavior is explained by the higher soil backscatter component at lower incidence angles, which translates in higher variability due to roughness and moisture. Light precipitation did not have large impact on the backscatter. The average backscatter level of the 2009.01.21 dataset was similar to the level observed for the datasets acquired under dry conditions. An explanation for the apparent lack of precipitation effects is the low rainfall quantity registered (2 mm on 2009.01.21 and 0.25 mm on 2009.02.12) and the soils of the area which are unable to retain water as a consequence of the high hydraulic conductivity. However, heavy rainfall (11 mm on 2009.03.04 and 2009.03.05 before the image acquired on 2009.03.06) and vegetation surface moisture (0.25 mm registered three hours before acquisition on 2009.02.12) caused higher average backscatter coefficients (0.5-1 dB) at both polarizations and for all burn severities especially on slopes tilted towards the sensor.

The effect of look geometry on the backscatter of burned areas is illustrated by two datasets (2008.12.19 and 2008.12.24) acquired four days apart at 40° and 25° look angles respectively. Figure 3 presents the average backscatter by burn severity levels of flat or near flat areas. The short acquisition interval and the stable weather conditions suggest that observed differences are due to the steeper viewing geometry of the image acquired on the second date.

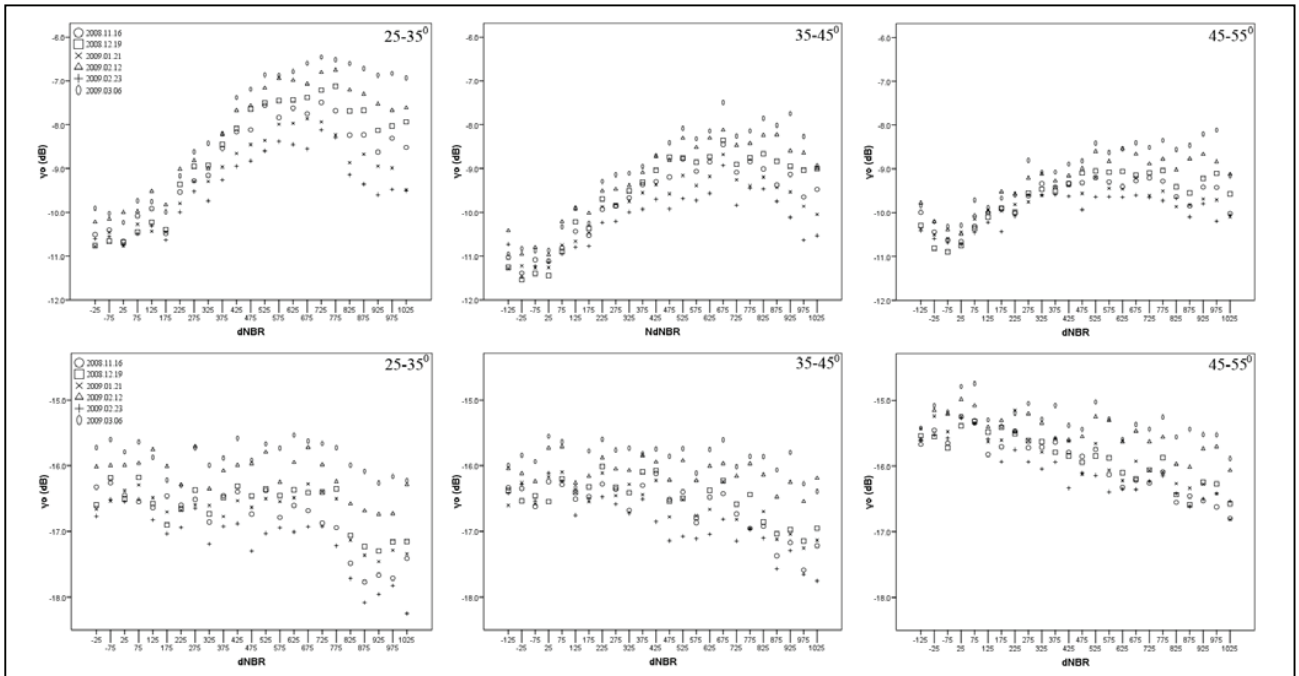

Fig. 2 Backscatter signatures for HH (top) and HV (bottom) polarizations for the six images acquired at 40° look angle. Measurements have been grouped for 10° local incidence angle intervals

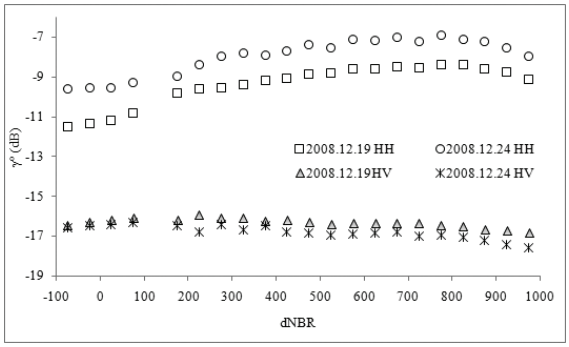

Fig.3 Backscatter with respect to dNBR for an image acquired with 40° look angle (2008.12.29) and 25° look angle (2008.12.24). Only pseudo-plots on flat or near flat areas are considered

The 2 dB higher values registered for HH polarization at all severity levels in the image acquired at 25° could be explained in terms of higher proportion of direct scattering from the ground at steeper incidence angles and the lower attenuation of the forest canopy. At HV polarization forest floor plays a less important role, which explains the much smaller backscatter difference.

4.2. Analysis of the association strength

Figure 4 illustrates the determination coefficient for all images processed at 25 m pixel spacing with multi-looking, without applying multi-temporal filtering (ENL equal to 55). The almost negligible effect of the weather conditions on the backscatter resulted in similar determination coefficients. No significant differences were noticed for data acquired at steeper look angle (2008.12.24) or for data acquired after light rainfall (2009.01.21 and 2009.02.12). However, for the image acquired after heavy rainfall (2009.03.06) a decrease of the determination coefficients was evident at higher local incidence angles. At these angles HV polarization accounts for a larger part of the variability explained by the regression model [6]. For the image acquired when vegetation was wet (2009.02.12) the dynamic range was smaller compared to the other images, which influenced the association strength to burn severity levels.

The use of larger plots eliminates variability due to speckle, increasing the association strength to burn severity. Figure 5 illustrates the influence of plot size on the association strength for the image acquired on 2008.12.19 processed to 10 m (ENL equal to 9) and to 25 m (ENL equal to 55). A marked increase of the determination coefficients with the number of pixels per plot is evident. For lower ENL, more samples within a plot are needed to obtain similar determination coefficients as for the data processed with stronger multi-look factors.

The effect of additional multi-temporal filtering is presented in Figure 6. To obtain different levels of speckle suppression before filtering the 2008.11.16 image was multi-looked with different factors (17×10 and 8×5). The images with 25 and 32 ENL were obtained after applying AdMTF to the 10 m spatial resolution data using 3 or 6 images respectively, while the images with 90 and 125 ENL were obtained after applying AdMTF to the 25 m spatial resolution data. The results suggest that when strong multi-looking factors (17×10) were applied, AdMTF improved little the retrieval of burn severity. At higher spatial resolution (10 m) the use of AdMTF greatly improved burn severity retrieval, higher R^2s (up to 0.2) being observed for the filtered images.

Nevertheless, doubling the number of images used for temporal filtering (from 3 to 6) did not improve significantly burn severity retrieval.

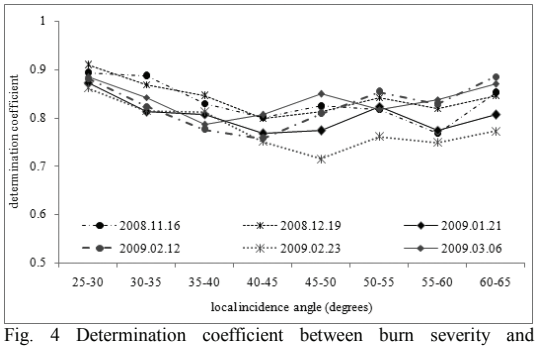

Fig. 4 Determination coefficient between burn severity and backscatter coefficient with respect to local incidence angle for images with ENL equal to 55 and 9 pixels per pseudo-plot

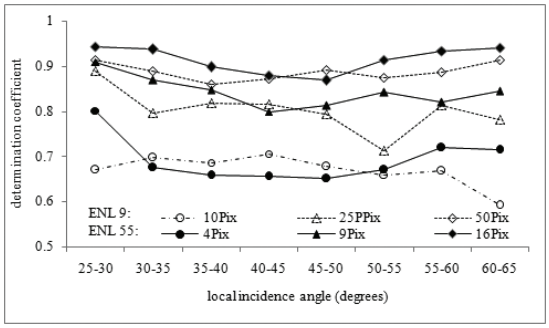

Fig. 5 Determination coefficient between burn severity and backscatter coefficient with respect to local incidence angle for the image acquired on 2008.12.19

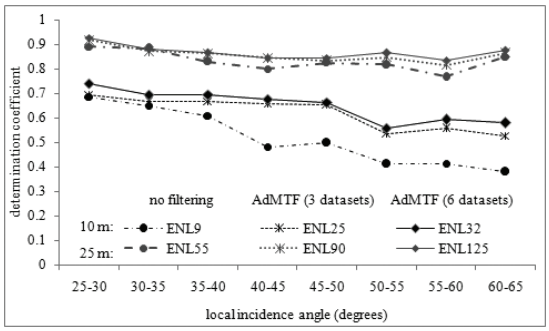

Fig. 6 The influence of speckle reduction on the association strength between burn severity and backscatter coefficient for 2008.11.16 dataset (9 pixels per plot)

5. CONCLUSIONS

In this paper several aspects concerning the use of multi-temporal dual-polarized (HH and HV) TerraSAR-X data for burn severity evaluation have been investigated. For unburned areas the backscatter showed temporal variability comparable to the declared radiometric accuracy (0.6 dB). With increasing burn severity the temporal variability of the backscatter increased reaching up to 2dB for highly burned areas on slopes oriented towards the sensor (HH-polarization). The high temporal stability provided consistent results in terms of burn severity evaluation. Evaluation of burn severity is possible up to nine months after fire. Light rain prior to image acquisition influenced backscatter marginally. The backscatter and the determination coefficients were practically unchanged with respect to image acquired under dry conditions. The backscatter level increased while the determination coefficients decreased for images acquired after heavy rainfall or when vegetation presented surface moisture. The look geometry strongly influenced the backscatter, especially at HH polarization, in form of an offset. Nonetheless the association strength between backscatter and burn severity did not change. For burn severity evaluation, multi-temporal filtered images provided better results than unfiltered images. The association strength between backscatter coefficient and burn severity increased with the increase of ENL for data processed at high spatial resolution. Nevertheless, determination coefficients for backscatter obtained from temporally filtered images using six datasets were not significantly different compared to the case of using three datasets. When high multi-looking factors were used MTF did not improve significantly the determination coefficients.

ACKNOWLEDGMENT

This work has been financed by the Spanish Ministry of Science and Education and the European Social Fund. TerraSAR-X data were provided by Deutsches Zentrum für Luft- und Raumfahrt (DLR) in the framework of LAN0464 project.

6. REFERENCES

[1] P.G. Simmonds, A.J. Manning, R.G. Derwent, P. Ciais, M. Ramonet, V. Kazan, and D. Ryall, "A burning question. Can recent growth rate anomalies in the greenhouse gases be attributed to large-scale biomass burning events?", *Atmospheric Environment* 39 (14), pp. 2513-2517, 2005.

[2] M.O. Andreae, and P. Merlet, "Emission of trace gases and aerosols from biomass burning", *Global Biogeochem. Cycles* 15 (4), pp. 955-966, 2001.

[3] C.H. Key, and N.C. Benson, *Landscape assessment (LA)*, U.S. Department of Agriculture, Forest Service, Rocky Mountain Research Station, Gen. Tech. Rep. RMRS-GTR-164-CD, Fort Collins, CO, 2006.

[4] E. Chuvieco, D. Riaño, F.M. Danson, and P. Martín, "Use of a radiative transfer model to simulate the postfire spectral response to burn severity", *Journal of Geophysical Research,* 111 (G04S09), doi:10.1029/2005JG000143, 2006.

[5] M. Gimeno, J. San-Miguel, P. Barbosa, and G. Schmuck, "Using ERS-SAR images for burnt area mapping in Mediterranean landscapes", *Forest Fire Research & Wildland Fire Safey*, 2002.

[6] M. Tanase, F. Pérez-Cabello, J. de la Riva, and M. Santoro, "TerraSAR-X data for burn severity evaluation in Mediterranean forests on sloped terrain", *IEEE Trans. Geosci. Remote Sensing*, accepted, 2009.

[7] U. Wegmüller, C. Werner, and T. Strozzi, "SAR interferometric and differential interferometric processing", IGARSS`98, Seattle, pp. 1106-1108, 1998.

[8] C. J. Oliver, and S. Quegan, *Understanding synthetic aperture radar images*, Artech House, 1998.

[9] L.M.H. Ulander, "Radiometric slope correction of synthetic-aperture radar images", *IEEE Trans. Geosci. Remote Sensing* 34, pp. 1115-1122, 1996.